Supplementary information

Insights into the Distinguishing Stress-induced Cytotoxicity of Chiral Gold Nanoclusters and the Relationship with GSTP1

Chunlei Zhang[1], Zhijun Zhou[1], Xiao Zhi[1], Yue Ma[1], Kan Wang[1], Yuxia Wang[2], Yingge Zhang[2], Hualin Fu[1], Weilin Jin[1], Fei Pan[1] and Daxiang Cui[1]*

1. Institute of Nano Biomedicine and Engineering, Key Laboratory for Thin Film and Microfabrication Technology of the Ministry of Education, Department of Instrument Science & Engineering, School of Electronic, Information and Electrical Engineering, Shanghai Jiao Tong University, 800 Dongchuan RD, Shanghai 200240, China.

Daxiang Cui, E-mail: dxcui@sjtu.edu.cn; Tel&Fax: +86 021-34206886

2. Institute of Pharmacology and Toxicology, Academy of Military Medical Sciences, 47 Taping Road , Peking 100850, PR China

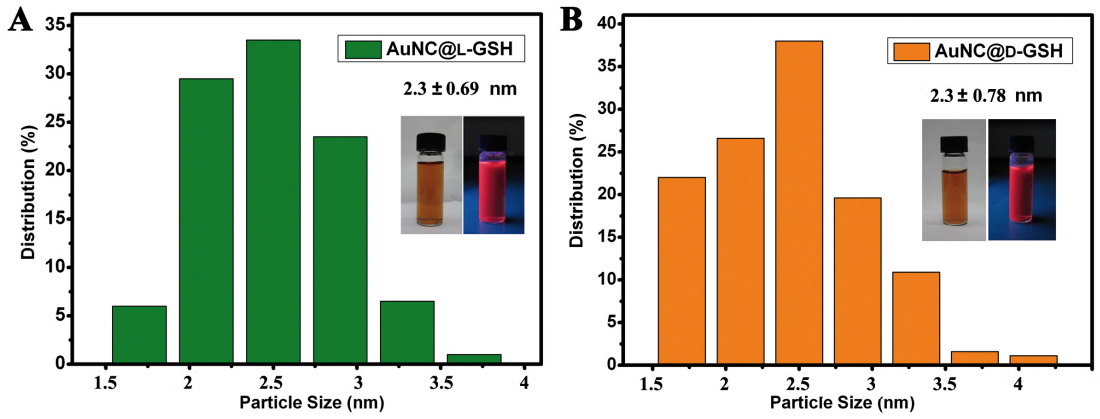

Figure S1. Size distribution of (A) AuNCs@L-GSH and (B) AuNCs@D-GSH. (Insets) Digital photos of (A) L-GSH- and (B) D-GSH-capped Au NCs under visible (left) and hand-held UV lamp (right) light (365 nm).

Table S1. Physicochemical properties of Au NCs

Au NCs	Surface modification	Dynamic diameter[a] [nm]	ζ-potential[b] [mv]
AuNCs@L-GSH	L-GSH	3.6±0.3	-12.5±0.4
AuNCs@D-GSH	D-GSH	3.7±0.4	-12.1±0.5

[a] The dynamic diameter of the Au NCs was the dynamic light scattering analysis of hydrodynamic diameter in aqueous solution; [b] The Zeta potentials of AuNCs were measured in aqueous solution of pH 7.0.

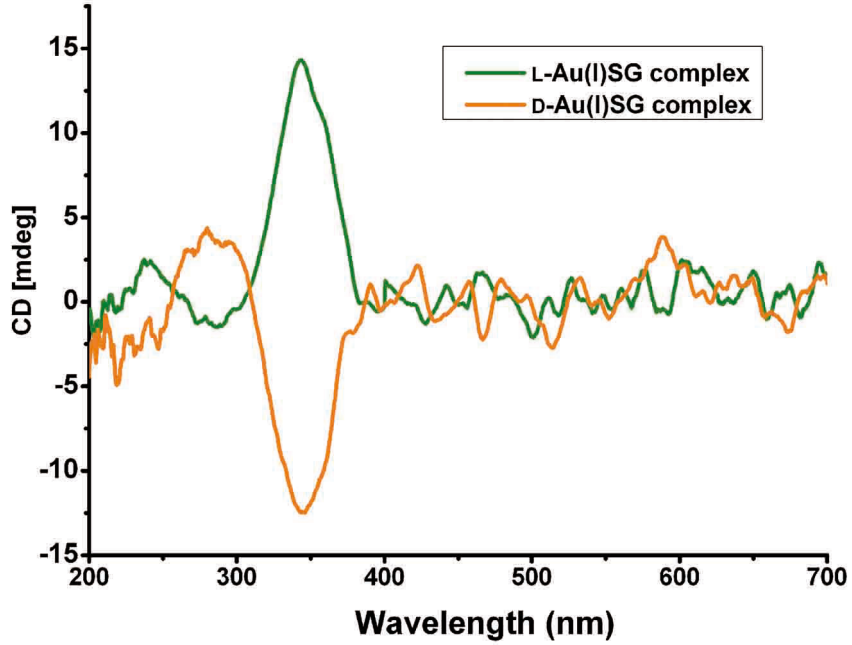

Figure S2. CD spectra of Au(I)-SG complexes. Note that SG represents glutathione in thiolate form.

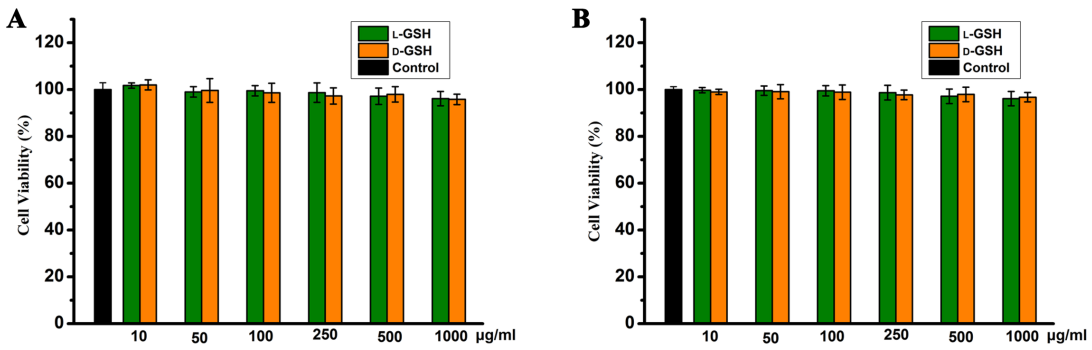

Figure S3. Cell viability of (A) MGC-803 and (B) GES-1 cells after co-incubation with different concentrations of L-GSH and D-GSH for 24 h.

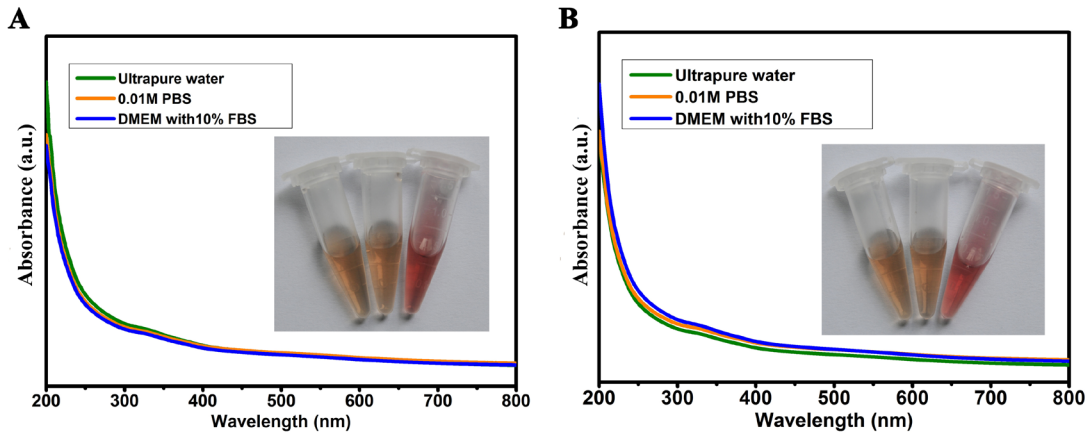

Figure S4. UV−vis absorption spectra (A) AuNCs@L-GSH and (B) AuNCs@D-GSH *in vitro*. (Insets) Digital photos of 1 mg/ml AuNCs@L-GSH and AuNCs@D-GSH in ultrapure water, 0.01M PBS and DMEM with 10% FBS (from left to right) for 24 h at 37 °C.

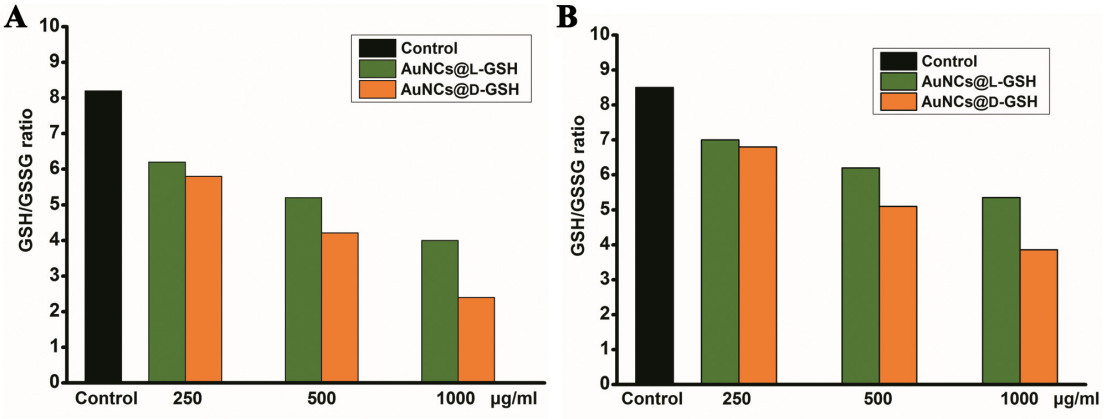

Figure S5. Intracellular GSH/GSSG ratio after Au NCs exposure. AuNCs@L-GSH and AuNCs@D-GSH significantly decreased the GSH/GSSG ratio in (A) MGC-803 and (B) GES-1 cells compared with untreated control, the data indicating a significant oxidative stress.

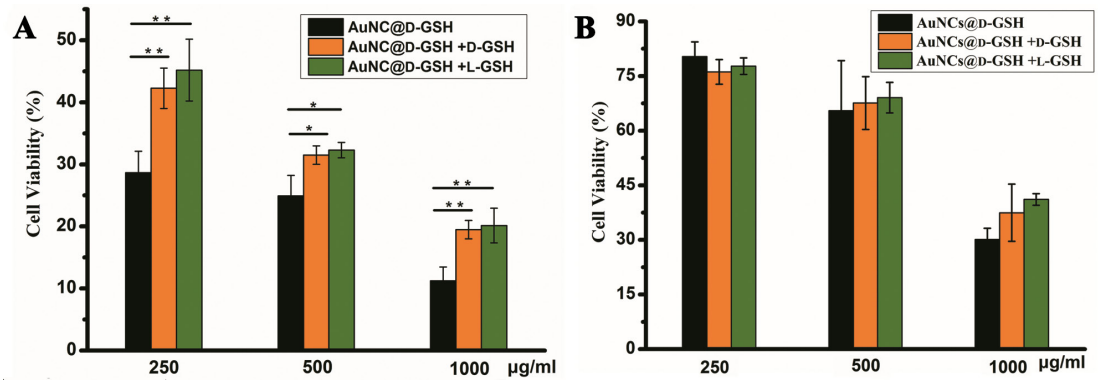

Figure S6. L-GSH and D-GSH can partially inhibit the cytotoxicity of AuNCs@D-GSH. (A) MGC-803 and (B) GES-1cells incubated with AuNCs@D-GSH at several different concentrations and mixed with L-GSH and D-GSH respectively for another 24 h co-incubation. *p<0.05, **p<0.01, Student's t-test results at 95% confidence level were significantly different.

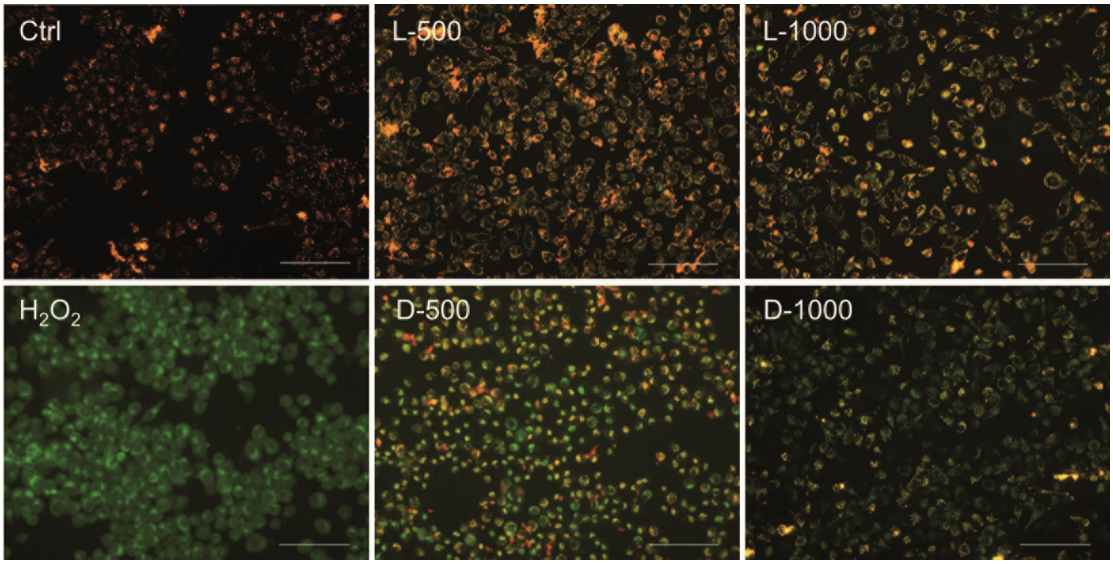

Figure S7. Fluorescent potential-dependent staining of mitochondria in GES-1 cells by JC-1 following exposure to Au NCs for 12 h. L-500, L-1000, D-500, D-1000 were denoted as GES-1 cells treated with 500 and 1000 μg/ml AuNCs@L-GSH, 500 and 1000 μg/ml AuNCs@D-GSH respectively. The cells were illuminated at 450-490 nm and the emission was collected with a 515 nm longpass optical filter. Scale bars: 100 μm.

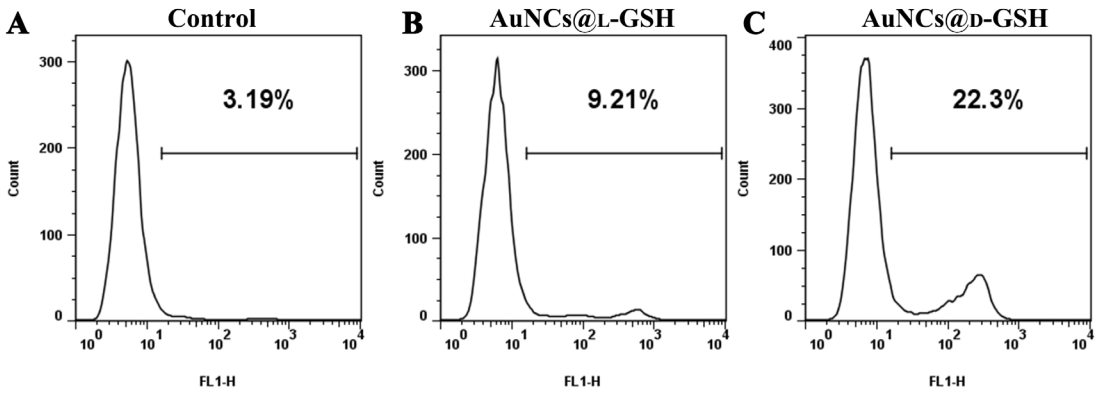

Figure S8. Flow cytometry analysis of the phosphorylation of H2AX. (A) GES-1 cells without any treatment. (B-C) GES-1 cells treated with 100 μg/ml AuNCs@L-GSH and AuNCs@D-GSH for 24, respectively.

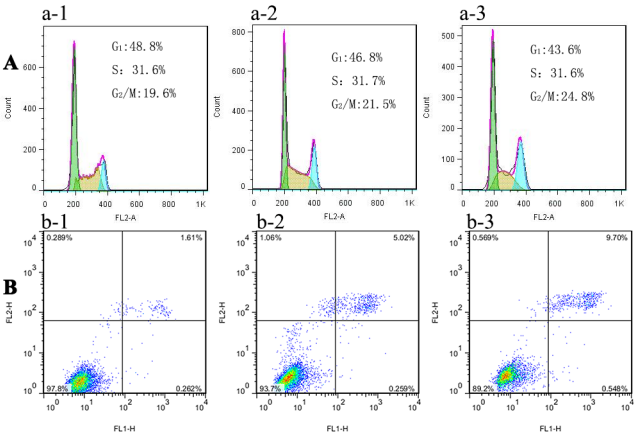

Figure S9. Flow cytometry analysis of (A) cell cycle phase distribution and (B) apoptosis/necrosis in GES-1 cells after exposure to (a-2, b-2) 100 μg/ml AuNCs@L-GSH and (a-3, b-3) 100 μg/ml AuNCs@D-GSH for 24 h, respectively. (a-1, b-1) Cells without any treatment.

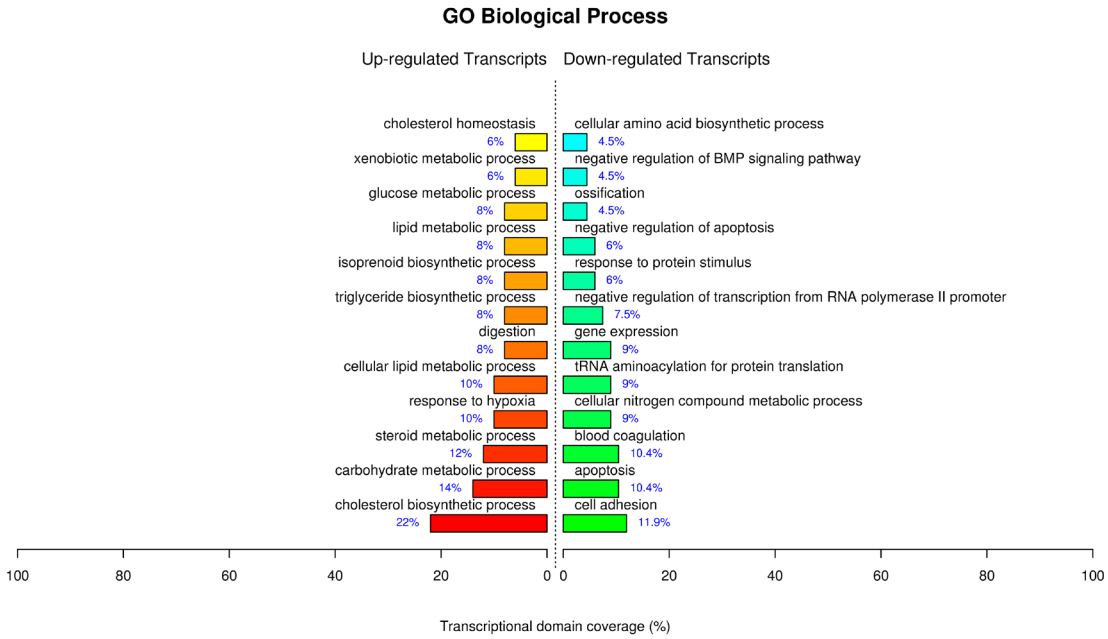

Figure S10. G0 terms of *biological process* significantly affected by AuNCs@D-GSH.